IL NUOVO CIMENTO **48 C** (2025) 36
DOI 10.1393/ncc/i2025-25036-y

COLLOQUIA: WPCF-Resonance 2023

The Pixelation strategy for the FARCOS array

G. CARDELLA[1](*), N. S. MARTORANA[1], L. ACOSTA[4][5], G. D'AGATA[3], E. DE FILIPPO[1], E. GERACI[3][1], B. GNOFFO[3][1], C. GUAZZONI[6], C. MAIOLINO[2], A. PAGANO[1], E. V. PAGANO[2], M. PAPA[1], S. PIRRONE[1], G. POLITI[3][1], F. RISITANO[7][1], F. RIZZO[3][2][8], P. RUSSOTTO[2], G. SANTAGATI[1], M. TRIMARCHI[7][1] and C. ZAGAMI[2][3][8]

([1]) *INFN, Sezione di Catania - Catania, Italy*
([2]) *INFN, Laboratori Nazionali del Sud - Catania, Italy*
([3]) *Dipartimento di Fisica e Astronomia "Ettore Majorana", Università degli Studi di Catania Catania, Italy*
([4]) *Instituto de Fìsica, Universidad Nacional Autónoma de México - Mexico City Mexico*
([5]) *Instituto de Estructura de la Materia, CSIC - Madrid Spain*
([6]) *DEIB Politecnico di Milano and INFN Sez. Milano - Milano, Italy*
([7]) *Dipartimento di Scienze MIFT, Università di Messina - Messina, Italy*
([8]) *CSFNSM, centro Siciliano di Fisica Nucleare e Struttura della Materia - Catania, Italy*

received 23 July 2024

Summary. — A novel pixelation method for the double sided silicon strip detectors of the FARCOS array has been developed and tested with the data collected at INFN-LNS laboratory. The reconstruction of two and three alpha particles coincidence events is shown. The need to use the detection time of each signal to clean the events from noise and spurious coincidences is underlined. The method is able also to reconstruct interstrip events and to exclude the degradation of the resolution generated by events interacting near the guard ring. The energy resolution of well reconstructed interstrip events was evaluated by looking at two alpha particles coincidences.

1. – Introduction

Double sided silicon strip detectors (DSSSDs) are very useful tools able to detect particles with a good energy and angular resolution. They are obtained by segmenting both front and back side electrodes in narrow orthogonal implanted regions each one separated by thin oxide regions. The particle detection angle is determined by the crossing point of the fired front and back strips. DSSSDs can cover a relatively large solid angle, therefore there is a not negligible probability to detect more than one particle in the same event, in the same DSSSD. In this case it is important to be able to assign to each front strip

(*) E-mail: cardella@ct.infn.it

the correct back strip. This is the pixelation job. Many arrays are available based on such kind of detectors, see for instance [1-3]. In the last years the FARCOS array [4] was built and it was installed at INFN-LNS. The FARCOS array uses, as first two stages of its 20 telescopes, two DSSSDs 300 μm and 1500 μm thick respectively. All detectors are segmented in 32x32 strips 2 mm pitch. In this contribution the pixelation method used in order to assign the correct detection angle to each particle will be shortly described.

2. – Timing and Pixelation analysis

The first operation performed during the data analysis process is the cleaning of the data by random events. The full digital electronics used [5] allow the digitization of all signals with a sampling rate of 50 MHz. The digitized signal is analyzed to derive the deposited energy, the hit time, the signal rise and fall times, and others. When more than one signal is collected in each DSSSD an analysis on the hit time is performed in order to ensure that all signals belong to the same event. Signals with a large time difference are discarded. Also signals with anomalous rise and fall times are usually discarded. A fast fall time of the signal for instance is observed in events induced in the more external strips (0 and 31) from particles impinging around the guard ring of the detector. This cleaning analysis is fundamental to perform a correct pixelation work.

2˙1. *Pixelation analysis.* – The pixel analysis is based on the fact that an impinging particle produces two equal signals, with opposite sign, in the front and back strips fired. Therefore once a good calibration is available the comparison of the energy associated to each signal should be enough to perform the correct association of the front and back strips needed to select the detection pixel. However, there are many difficulties in the application of this relatively simple principle. First, the energy resolution can influence the choice of the correct association of front and back strips; second, interstrip events with the sharing of energy between two adjacent strips caused by the electric field distribution in the middle of the two strips make also difficult the association of front and back signals. The energy sharing of interstrip events can be further perturbed by the energy threshold that may prevent the acquisition of one of the two contributions, by malfunctions of one of the strips, and, in some cases, also by induction phenomena. To overcome the problem, a minimization routine is used computing for each possible choice of the front-back strips the energy difference of the associated couple, and searching for the minimum of the Total Energy Difference (TED) of the event.

2˙2. *Example of data treatment.* – In order to better clarify the procedure used the analysis of a real event reported in table I can be performed.

TABLE I. – *Example event with apparent multiplicity 3.*

side	strip	Time (ch)	Energy(MeV)
front	1	86.07	6.961
front	8	84.92	22.045
front	9	60.48	12.516
back	17	84.01	16.849
back	18	83.04	5.796
back	28	83.43	7.059

In this event only the 300 μm thick DSSSD was hit. 3 signals were measured in the front side, and another 3 in the back side, therefore it is an event with apparent multiplicity 3. Table I reports the detector side, the strip number, the detection time in channels (20 ns per channel), and the energy detected in MeV. The detection time of most of the signals is around channel 84, while the detection time of the front strip 9 is around channel 60. This signal arrived about 480 ns before the other signals; it is a random coincidence that must be excluded by the event. In this way, the occurrence of an interstrip event in the front side between the strips 8 and 9 is also excluded. Only two front signals survive after the time analysis, therefore the event is composed by no more than two real particles (a particle is defined by the intersection of a front and a back signal). The strip numbers in the back side are 17, 18 and 28, it is possible that the signals in the strips 17 and 18 are produced by a single particle impinging in the interstrip region. To decide if this is a real interstrip, it is not enough the fact that in the front side there are only two good signals. All the possible couplings of signals into two particles must be evaluated to perform the correct choice. There are 6 possible combinations of the two front strips with the 3 back ones, moreover there are two other combinations between front and back strips assuming that the strips 17 and 18 are generated by an interstrip event. For all these 8 particle combinations we can evaluate the TED, defined as follows:

$$TED(k) = \Sigma_j^n |E_{front}(j,k) - E_{back}(j,k)| \tag{1}$$

Where $E_{front}(j,k)$ and $E_{back}(j,k)$ are respectively the energies measured in the front and back strips, tentatively coupled in the k choice, to define the detection position of the j-particle. The sum is over all the possible well reconstructed n particles of the event, 2 in this case. While there are 8 possible k combinations, calculations can be simplified excluding by default all the combinations between couples of front and back strips with very large energy difference as strip front 1 ($\approx$ 7 MeV) with strip back 17 ($\approx$ 17 MeV). Only 3 combinations survive from this preliminary selection. The minimum TED is found at 0.7 MeV, coupling the front strip 1 with the back strip 28 and the front strip 8 with the back interstrip event 17-18. In conclusion we have selected two particles respectively of $\approx$ 7 MeV and $\approx$22 MeV. In this event the data treatment adopted was able to exclude the presence of a front interstrip and to reduce the true multiplicity from 3 to 2 particles.

3. – Results

The analysis of the signals detection time, the pixelation algorithm with the rejection of uncoupled front-back signals, and the recovery of interstrip events, allow a significant improvement in the identification performance of the scatter plots collected in the measurement and a simplification of the data analysis. Figure 1 shows two examples that show the efficacy of the data analysis procedure. The upper panels report the identification ΔE-E scatter plot (panel a) and the plot of the energy detected in coincidence into two adjacent strips of a detector (panel (b)). These plots were built using data from the ^{4}He+^{12}C reaction at 64 MeV performed at INFN-LNS [6, 7]. These "raw" events were scatterplotted before both the time cleaning and the pixelation phase. The identification ΔE-E plot show a sufficient identification capability: the lines of hydrogen and helium isotopes can be observed well separated one by the other. However, many signals spread in the region between the identification lines and in particular below the

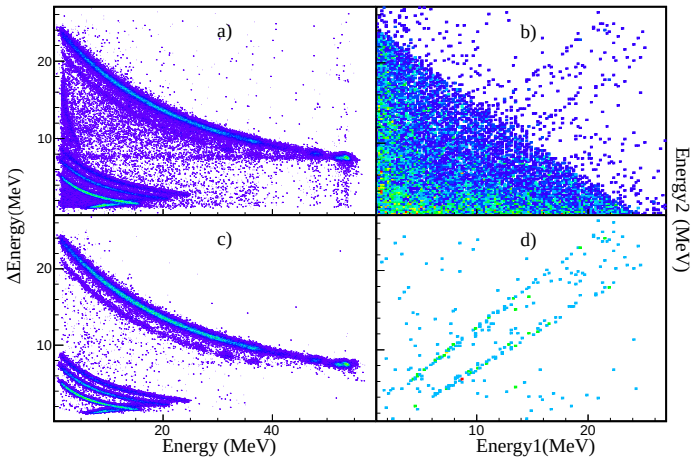

Fig. 1. – (a) ΔE-E identification scatter plot, raw, energy calibrated data; (b) raw, calibrated energy correlation plot of two signals measured in coincidence into two adjacent strips; (c) same as (a) after the complete pixelation work; (d) same as (b) after the complete pixelation work.

proton line, where many unidentifiable events can be observed. An unknown line is also present in the region between hydrogen isotopes and helium isotopes below 5 MeV of energy detected in the E stage. The adjacent strip energy plot of panel (b) shows a low-left triangular region with a maximum energy around 23 MeV full of events. Along the down-left top right diagonal of the plot some lines can be also noted. In panels (c) and (d) the effect of the time cleaning and pixelation work can be seen. In panel (c) the ΔE-E plot after the two data analysis stages is shown. All the misidentified lines observed in panel a) are now absent. Nearly all the "fog" between the isotope lines is cancelled, the relevant noise concentration below the proton line is absent. Most of the distributed fog and the noisy region under the proton line were due to interstrip events. After the reconstruction of these events the correct energy is obtained and almost all events go into the proper isotopic line.

In panel (d) all the events of the triangular region due to interstrip events were removed and the two lines that were partially hidden in panel (b) can be now well seen down to the low energy region. They are the kinematic locus of the $^{8}Be_{g.s.}$ decay into two α-particles [8].

Figure 2(a) shows the center of mass excitation energy of two α-particles detected in coincidence. The $^{8}Be_{g.s.}$ resonance at 92 keV is shown with an RMS energy resolution of 6.7 keV thanks to the very good performance of the pixelation job. Figure 2(b) shows the Hoyle state resonance of ^{12}C at 7.64 MeV measured from the triple α-particles coincidence. 40% of the collected statistics of this last spectrum is due to the proper recovery of interstrip events and coincidences between adjacent front or back strips showing again the quality of the job performed.

4. – Conclusions

In this paper we present the strategy designed for the FARCOS array in order to assign the correct detection angle to each particle. The applied method allows one to recover

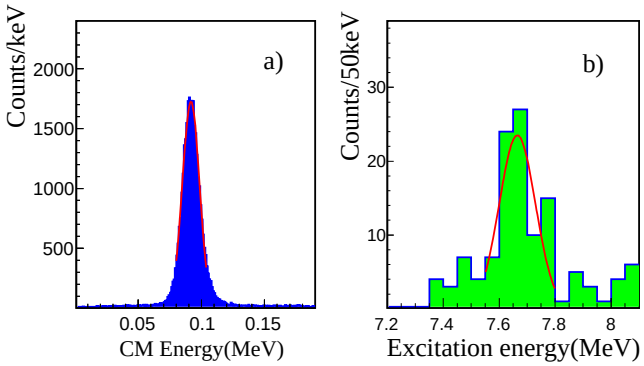

Fig. 2. – (a) Center of mass energy spectrum of two coincidence α-particles; (b) excitation energy spectrum of ^{12}C computed from the center of mass energy of 3 coincidence α-particles.

also multi-particle coincidences. A multiplicity 3 event was presented as an example of the reconstruction mode. Even events with higher multiplicity were successfully analysed. The method allows the discrimination between interstrip and true coincidence events when two adjacent strips collect charge at the same time. The FARCOS array will be soon used also with radioactive ion beams that will be available at LNS with the new FRAISE facility now under construction [9, 10]. The correct choice of the impact point coupled with a precise positioning laser system [11] allows one to reach excellent energy resolutions in particle-particle correlation measurements as shown in fig. 2(a) for the $^{8}\mathrm{Be}_{g.s.}$ 2 α-particles decay. The extension of this data analysis method to novel pixel detectors presently under construction in the framework of the Samothrace project is on going [12].

* * *

This work has been partially funded by the DGAPA-UNAM IG101423 and CONACYT 315839 grants, by the "Programma ricerca di Ateneo UNICT 2020-22 linea 2", and by European Union (NextGeneration EU), through MURPNRR project SAMOTHRACE (ECS00000022).

REFERENCES

[1] Wallace M. *et al.*, *Nucl. Instrum. Methods Phys. Res. A*, **583** (2007) 302.
[2] Kundu S. *et al.*, *Nucl. Instrum. Methods Phys. Res. A*, **943** (2019) 162411.
[3] Guan F. *et al.*, *Nucl. Instrum. Methods Phys. Res. A*, **1011** (2021) 165592
[4] Pagano E. V. *et al.*, *EPJ Web of Conferences*, **117** (2016) 10008.
[5] Pollacco E. *et al.*, *Nucl. Instrum. Methods Phys. Res. A*, **887** (2018) 81.
[6] Cardella G. *et al.*, *Phys. Rev. C*, **104** (2021) 064315.
[7] Cardella G. *et al.*, *Nucl. Phys. A*, **1020** (2022) 122395.
[8] Cardella G. *et al.*, *Eur. Phys. J. Plus*, **138** (2023) 89.
[9] Russotto P. *et al.*, *J. Phys.: Conf. Ser.*, **1014** (2018) 012016.
[10] Martorana N. S. *et al.*, *Front. Phys.*, **10** (2022) 1058419.
[11] Trifiró A. *et al.*, LNS report 2020 (2021) 79.
[12] `https://samothrace.eu/`.